

Electronic Supplementary Information (ESI)

Exploring the potential of exfoliated ternary ultrathin Ti_4AlN_3 nanosheets for fabricating hybrid patterned polymer brushes

Qun Ye^{#a}, Peng Xiao^{#a}, Wulong Liu^a, Ke Chen^a, Tao Chen^{*a}, Jianming Xue^b, Shiyu Du^a, Qing Huang^{*a}

^a Ningbo Institute of Material Technology and Engineering, Chinese Academy of Science, Ningbo, 315201, People's Republic of China.

^bState Key Laboratory of Nuclear Physics and Technology, Peking University, Beijing, 100871, People's Republic of China.

* Corresponding author:

E-mail: tao.chen@nimte.ac.cn

E-mail: huangqing@nimte.ac.cn

Postal address: No.1219 Zhongguan West Road, Zhenhai District, Ningbo City, Zhejiang Province, China, 315201.

Experimental Section

Preparation of Ti_4AlN_3 free-standing disc and Langmuir–Blodgett (LB) film:

About 150 mL Ti_4AlN_3 ink was dried in vacuum at 50 °C. The obtained powders (*ca.* 0.08g) were then filled into a stainless steel mould ($D = 8$ mm), and cold-pressed at 15 MPa for 1 min. The thickness of the as-pressed disc was about 500 μm . The self-assembled transparent film was prepared following the procedures introduced by Ref. [1].

Characterization: The phase composition of samples before and after immersion was analysed by X-ray diffraction (XRD), using a diffractometer (D8 Advance, Bruker AXS, Germany) with CuK_α radiation. The scan range (2θ) and step were set to 5°-65° and 0.02°, respectively. The microstructures of the treated samples were characterized by scanning electron microscope (SEM) (FEI Quanta 250 FEG, Hillsboro, OR). The transmission electron microscopy (TEM) and high-resolution TEM images were carried out on a FEI Tecnai F20 field emission electron microscope at an acceleration voltage of 200 kV. Atomic force microscopy (AFM) study in the present work was taken by a multimode AFM (Being Nano-Instruments, Ltd) operating in the contact and/or tapping mode using silicon cantilevers (spring constant: 0.15 Nm^{-1} , resonant frequency: 12 KHz for cantilever of contact mode, spring constant: 3~40 Nm^{-1} , resonant frequency: 75~300 KHz for cantilever of tapping mode). Raman spectroscopy of the samples was carried out on a microspectrometer (inVia-reflex, Renishaw, Gloucestershire, UK) using an Nd laser (532 nm) and a grating with 1800 lines mm^{-1} . Fourier Transform infrared (FTIR) Spectroscopy (Nicolet 6700, Thermo scientific, USA): Absorbance spectra were collected using a spectral resolution of 4 cm^{-1} at room temperature over a frequency range of 4000-400 cm^{-1} . Conductivity of the cold-pressed, free-standing Ti_4AlN_3 disc was test by a ST-2258A multifunction digital four-probe tester (Suzhou Jingge Electronic Co., Ltd), the distance between probes was 1 mm.

Results

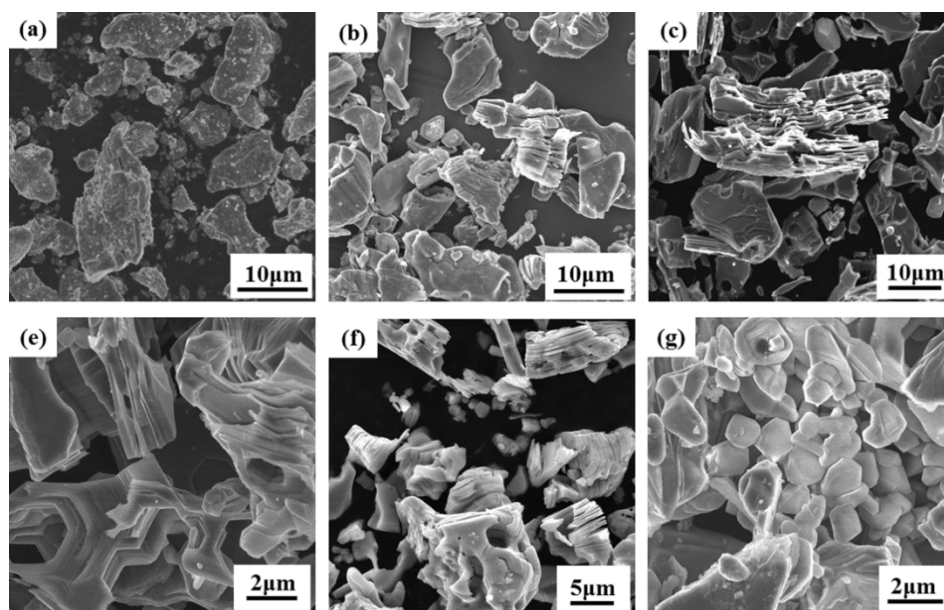


Figure S1. SEM images of Ti_4AlN_3 particles before and after etching treatment. (a) before etching, (b) etching in 10 wt. % HF for 108 h, (c) etching in 20 wt. % HF for 30 h, (d) etching in 25 wt. % HF for 30 h, (e) etching in 40 wt. % HF for 1.5 h, (f) etching in 40 wt. % HF for 30 h.

The Ti_4AlN_3 powders were immersed in HF solution with different concentration and etching time to find a suitable etching condition. SEM images of Ti_4AlN_3 particles before and after treatment were shown in **Figure S1**. Before etching, the particles are complete without gap between layers (**Figure S1a**). However, the particles become broken after etching, and some of them exhibit MXene-like structure (**Figure S1b - f**). In addition, many holes occur on the surface of Ti_4AlN_3 grains (**Figure S1c - f**), and make the grains incomplete. When the concentration of etchant is high and the etching time is long enough, the big Ti_4AlN_3 particles change into another kind of particles with a diameter less than 2 μm (**Figure S1g**). These results indicate a strong reaction happening between Ti_4AlN_3 phase and HF, and the reaction has weakened the bonds between Ti_4AlN_3 layers.

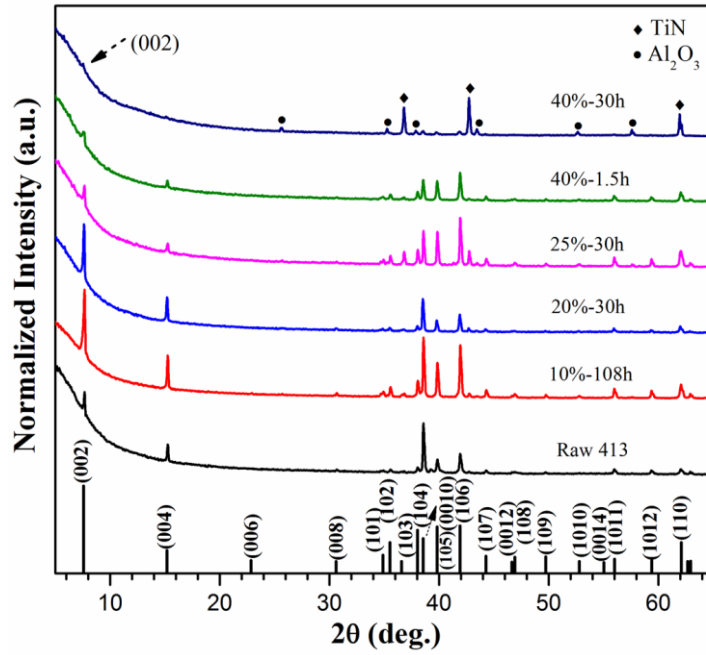


Figure S2. The corresponding XRD patterns of Ti_4AlN_3 particles before and after etching treatment at different conditions.

XRD pattern of raw powders shows a nearly pure Ti_4AlN_3 phase with negligible TiN impurity. After etching at low concentration or short time, the major phase in the powders is still Ti_4AlN_3 , but the relative intensity of peaks has changed, especially that of (002) peak. After etching in 40 wt. % HF for 30 h, the Ti_4AlN_3 phase nearly vanishes, only TiN and Al_2O_3 impurities left. Generally, the intensity of (002) peak is used to characterize z-orientation of MXene. To avoid the vanishing of (002) peak, the concentration to etch Ti_4AlN_3 phase should be lower than 25 wt. %, hence, 20 wt. % HF is considered as a suitable etchant.

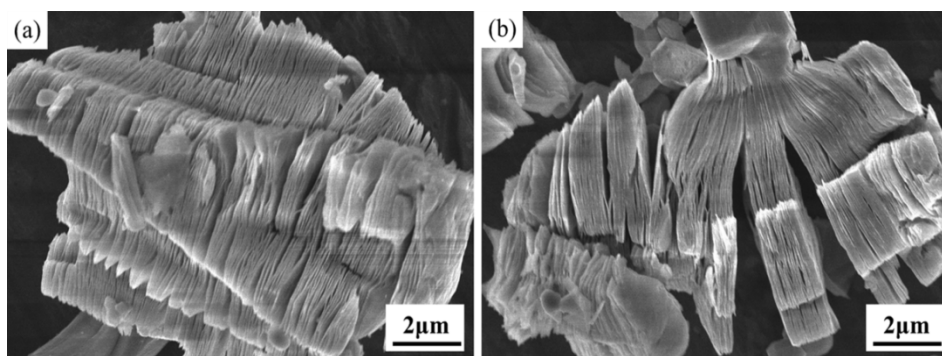


Figure S3. SEM images of etched Ti_4AlN_3 particles, showing typical MXene-like structure.

Part of as-etched Ti_4AlN_3 particles exhibit MXene-like structure, indicating the weakly bonding between the sheets.

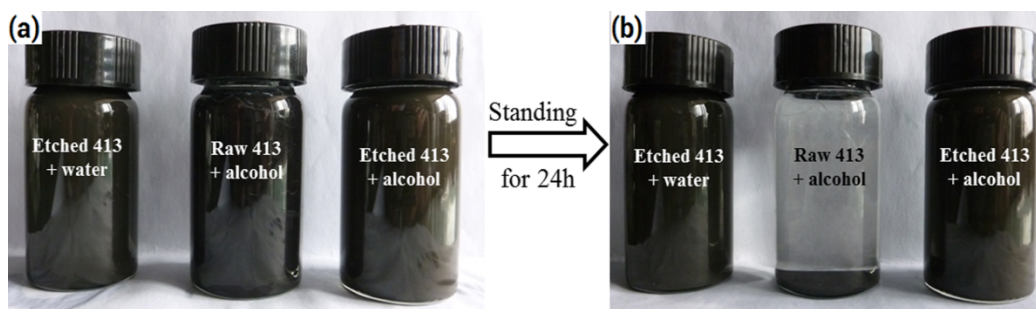


Figure S4. Digital photograph for different powders dispersed in water or alcohol (a) after sonication for 6 h, and (b) after standing still for 24 h. The graphs show that the as-etched Ti_4AlN_3 powders have good dispersibility in water or alcohol after sonication.

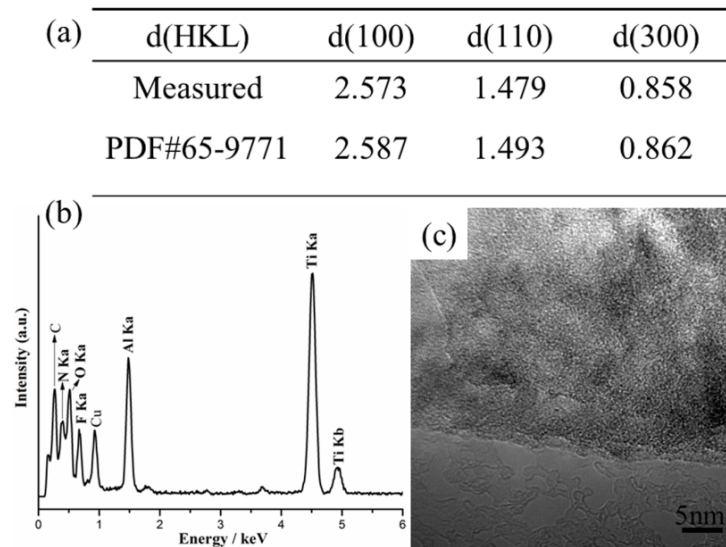


Figure S5. (a) The comparison between the measured and the standard interplanar spacing for Ti_4AlN_3 crystal.* (b) The corresponding EDS analysis of a typical nanosheet, indicating the existence of Ti_4AlN_3 phase with -OH, -F groups. (c) HRTEM image of a typical nanosheet, showing the structure of three layers. (* The standard interplanar spacing of (100) plane is calculated as $\sqrt{3}a/2$ ($a=2.988 \text{ nm}$)³ according to Ti_4AlN_3 crystal structure, and the unit in the table is *nm*.)

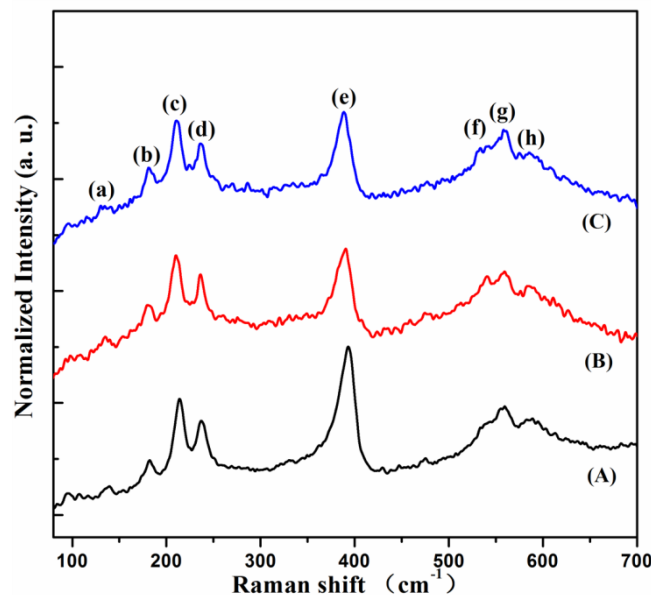


Figure S6. Raman spectra for Ti_4AlN_3 before (A) and after (B) 20 wt. % HF etching treatment, and for the exfoliated sheets film (C). All the Raman peaks ((a) – (h)) belonging to Ti_4AlN_3 phase still remain after etching or sonication, confirming the existence of Ti_4AlN_3 sheets.



Figure S7. Digital photographs of the cold-pressed, free-standing Ti_4AlN_3 disc with a diameter of 8 mm and a thickness about 0.5 mm. The resistivity of disc, measured by a four-probe tester, is only ca. $1.4 \, \Omega/\square$, indicating the good conductivity of this material.

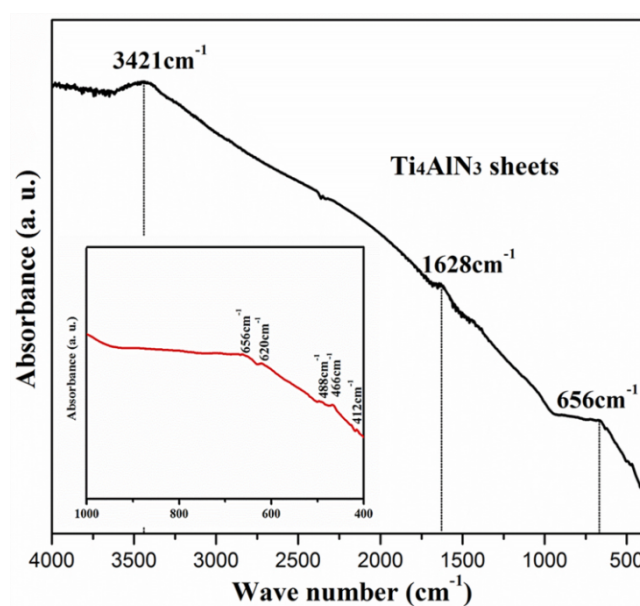


Figure S8. FTIR spectra of Ti_4AlN_3 sheets. The broad peak at $3421 \, \text{cm}^{-1}$ indicates the existence of hydroxyl group.

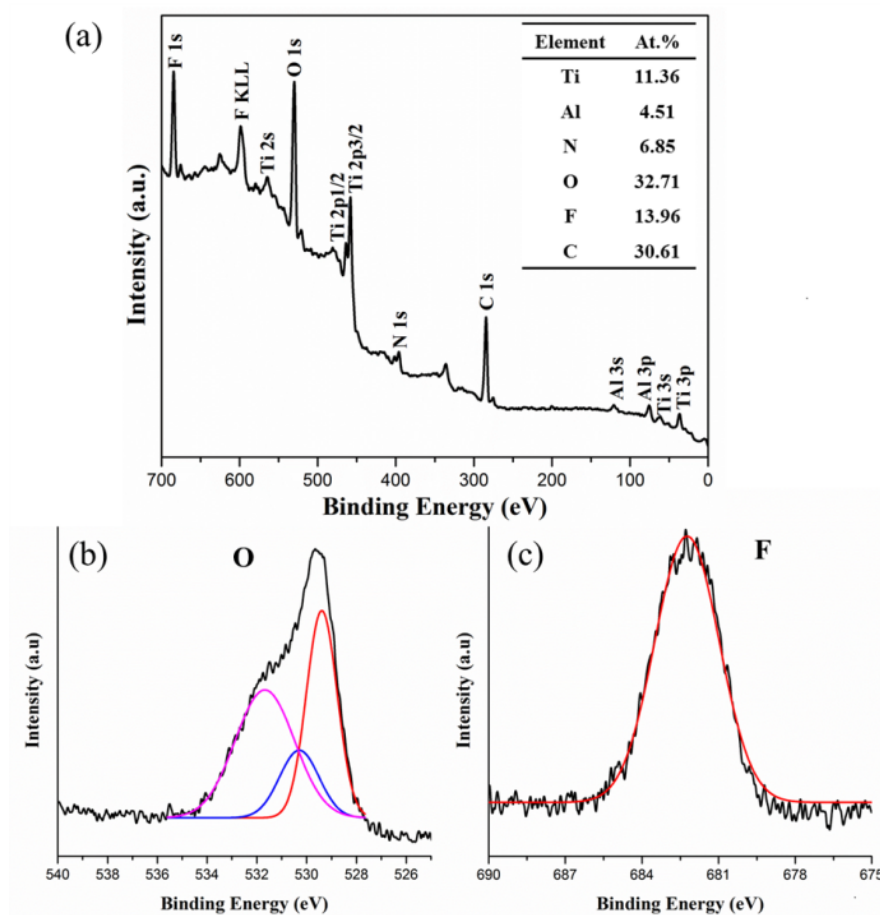


Figure S9. XPS spectra of as-exfoliated Ti_4AlN_3 nanosheets. (a) The full scan spectra, (b) O 1s region, and (c) F 1s region. Inset in (a) is a quantitative calculation of element content in the as-obtained nanosheets. The large amount of contamination (e.g. C) and low intensity of the Ti_4AlN_3 signal is due to the lack of Ar sputtering.

A high-resolution spectrum in the O 1s region (**Figure. S9b**) can be fit by peaks at 529.6, 530.5 and 531.9 eV. The component centered near 530.0 eV (529.6 and 530.5 eV) may be consistent with oxygen in different metal oxides. The component centered at 531.9 eV likely arises from O or OH groups bound to the surface of the Ti_4AlN_3 layers. The high-resolution spectrum in the F 1s region (**Figure. S9c**) also indicates the existence of abundant F group on the surface of the sheets.

Table S1. Measured Raman peak energies ω_{expt} for Ti_4AlN_3 sheets and corresponding calculated peak energies, and symmetries for the assigned modes in Ti_4AlN_3 .⁴

Mode	ω_{expt}	ω_{calc}	Irrep.
(a)	136	135	E_{2g}
(b)	181	172	E_{2g}
(c)	210	196	E_g
(d)	236	226	E_g
	-	248	E_g
	-	255	A_g
(e)	388	374	A_g
(f)	541	584	E_{2g}
(g)	560	587	A_g
(h)	585	600	E_{2g}

Reference

1. L. B. Liu, H. J. Kim and M. Lee, *Soft Matter*, 2011, **7**, 91-95.
2. I. Amin, M. Steenackers, N. Zhang, A. Beyer, X. H. Zhang, T. Pirzer, T. Hugel, R. Jordan and A. Golzhauser, *Small*, 2010, **6**, 1623-1630.
3. S. Myhra, J. A. A. Crossley and M. W. Barsoum, *J. Phys. Chem. Solids*, 2001, **62**, 811-817.
4. J. E. Spanier, S. Gupta, M. Amer and M. W. Barsoum, *Phys. Rev. B*, 2005, **71**.